



Wind-Induced Ventilation Based on the Separated Flow Region

M. Rahimi^{1†} and M. Javadi Nodeh²

¹ Associate Prof., Department of Mechanical Engineering, University of Mohaghegh Ardabili, Ardabil, Iran
² M.Sc. Student, Department of Mechanical Engineering, University of Mohaghegh Ardabili, Ardabil, Iran

†Corresponding Author Email: rahimi@uma.ac.ir

(Received January 8, 2014; accepted December 28, 2014)

ABSTRACT

An experimental investigation was conducted to study the potential use of the pressure reduction within the separated flow region followed by the wake at the leeward direction of a solid surface in natural ventilation of buildings. Air flow with mean velocity up to 7 m/s was directed onto a solid surface (circular plate and a semi-spherical surface) behind which the top end of a vertical vent pipe had been placed. Pressure reduction at the exit section of the pipe, which was well inside the separated flow region, induced an air flow within the pipe. This air flow rate from the stagnant surroundings into the wake region was measured under different geometrical configurations and for various wind velocities. The study revealed that the pressure reduction within the separated flow region would be applicable for natural ventilation of different spaces at least as an auxiliary system. The spaces include; sanitary places, crop protection stocks, industrial workshops and other spaces where no regular ventilation is required.

Keywords: Natural ventilation; Separated flow region; Wind energy.

NOMENCLATURE

C_p	pressure coefficient	V	mean velocity of air within the vent pipe
D	diameter of the semi sphere	x, y, z	cartesian coordinates
d	diameter of the vent pipe (m)	μ	dynamic viscosity of air at laboratory condition
Q	volumetric ventilation flow rate (m^3/s)	I_p	density of air at laboratory condition
Re	Reynolds number		
U	mean artificial wind velocity (m/s)		

1. INTRODUCTION

Ventilation of buildings could be accomplished both by forced and natural ventilation methods. In the first category, air displacement is mainly achieved using a fan which consumes electrical energy. Temperature or pressure differences between indoor and outdoor of a building originating from a renewable energy source gives rise to air displacement in the second category. The temperature difference causes the stack effect in which indoor warm air exits from the upper openings of a building replacing with the outdoor fresh air from the lower openings. Wind-induced natural ventilation is based on a pressure difference created by the wind and various types of its operation and mode of engagement are found in the published literature.

Mochida *et al.* (2005) experimentally demonstrated that the indoor thermal comfort could be improved

by utilizing cross-ventilation in which the window opening is controlled. Karava *et al.* (2007) studied wind-driven cross-ventilation in a building caused by sliding window openings placed on two adjacent walls. They found that the discharge coefficients vary considerably with the opening area and the inlet to outlet ratio. Based on the experimental results, they also determined that the pressure and the velocity fields would be unsteady particularly in the case of cross-ventilation with large opening areas. Chiu and Etheridge (2007) studied envelope flow models which are used in the design of naturally ventilated buildings. Modification for the discharge coefficient of the openings as the main parameter in the employing of the models was suggested due to the unsteadiness in both the flow and pressure fields. They concluded that the effect of the external flow fluctuations would be negligible when the outlet of a long opening such as a chimney lies within the external flow. Li and Mak (2005) conducted a numerical study to examine the

performance of a wind catcher. They concluded that the wind catcher performance was greatly influenced by the external wind speed and direction with respect to the wind catcher quadrants. The maximum velocity of air entering the room was close to the external wind speed and the wind catcher system in addition was found to be an efficient way to channel fresh air into the room. Mak *et al.* (2005) studied the ventilation performance of a wing wall numerically. They found that the wing wall could promote natural ventilation by increasing the air change per hour at various wind speeds and wind directions. Chu *et al.* (2010) investigated wind-driven cross ventilation in partitioned buildings using wind tunnel experiments. Based on their findings, the ventilation rate increased as the internal porosity became larger and the maximum ventilation rate occurred when the windward and leeward opening areas were equal. Also, they concluded that the ventilation rate of partitioned buildings was always smaller than that of buildings without partition. Hughes and Cheuk-Ming (2011) studied the relationship between external wind and buoyancy effect in an established flow through a wind tower. Based on their findings, the effect of buoyancy would be insignificant without an external air flow passage, such as a window, other than the wind tower itself. Based on an empirical study, Haw *et al.* (2012) concluded that a wind tower has potential use to improve the indoor air quality for buildings in the hot and humid climate. Aldawoud and Clark (2008) investigated the energy performance of a central atrium compared to a courtyard under the same geometrical proportions. The results of the study showed that the open courtyard building exhibits a better energy performance for the shorter buildings. However, the enclosed atrium exhibited a better energy performance as the building height was increased. They proposed that this trend was due to the contribution of different parameters including glazing and other climate parameters. Khan *et al.* (2008) presented measurements of flow rates by four commercial turbine ventilators on a specifically designed experimental system. The ventilators flow rates were taken at different wind speeds and compared with a simple open column and two standard vent hats. Lai (2006) developed a prototype of the rooftop turbine ventilator powered by hybrid wind and photovoltaic energy. Using a low-speed wind tunnel experiment, he suggested that the ventilation rate was improved by installing an inner fan at low outdoor wind speed (0 – 5 m/s). Also, a rated rotation speed close to 1500 rpm was highly recommended when installing the inner fan. Adekoya (1992) examined the performance characteristics of a rotating suction cowl. A suction rotating cowl was installed on the roof of a farm building and the developed static pressure was measured for various wind speeds. For the range of examined wind speeds, very low static pressure was reported. Therefore, it was proposed that a parallel arrangement of a number of cowls would be required for applications. An extensive review is also found for the wind driven ventilation techniques in the literature (Khan *et al.* 2008). All the wind-induced ventilation techniques, which are

used in low energy building design, have been classified as passive, directed passive and active methods in that review article. The methods in which wind-induced effects are directly used as motive forces for providing ventilation are referred as passive methods. Window openings, atria and courtyards, wing walls, wind catcher and wind towers are examples from the passive method. Devices used in the passive method have generally no moving parts although some moving or controlling additions have been integrated in recent modifications. Wind cowl and wing Jetter system are two devices which are classified in the second category. These devices are generally used in the roof ventilating structure. They could be stationary or rotate about an axis so as to always have the opening in appropriate position to the incident wind. In a suction cowl, the opening faces back the wind to develop a negative pressure for air extraction and in a wing Jetter system, air flow accelerates on the under-side of the system thus causing a negative pressure which exhausts air. Turbine ventilators and rotating chimney cowl are examples from the active wind-induced ventilation methods.

Wind incident on a solid surface such as a disk or a semi-sphere will produce a separated flow region followed by a wake at the leeward side of the surface. The pressure within this region will be lower than the surroundings pressure. It is seen from the existing literature that the potential use of the pressure difference between the indoor of a building and the wake region produced at the top end of a vent pipe in wind-induced ventilation has been given less attention. Therefore, the specifications of the pressure field established within the wake and the induced flow was investigated at the present study. For this purpose, a simple solid surface connected to the top end of a vertical pipe and it was exposed to a controlled air stream at a system. An air flow was developed within the pipe due to the pressure difference between the bottom and top ends of the pipe. The air flow rate was determined for various geometrical shapes and configurations which are described in the following sections.

2. MATERIALS AND METHODS

In order to make a sense of the pressure reduction within the wake, a simple test was conducted using a low-speed small wind-tunnel. As indicated in Fig. 1, a semi-spherical surface having 65 mm diameter and made from stainless steel sheet was fixed within the tunnel and in front of an air flow. A number of equally spaced pitot-tubes were placed at the leeward of the surface and at different positions to measure the local stagnation pressure. One excessive pitot-tube was also employed for measuring the static and the stagnation pressure difference, based on which the velocity of the flow was determined. Each of the measuring tubes was individually connected to a piezometric tube by a flexible pipe and the local pressure was measured and recorded in millimeter of water column.

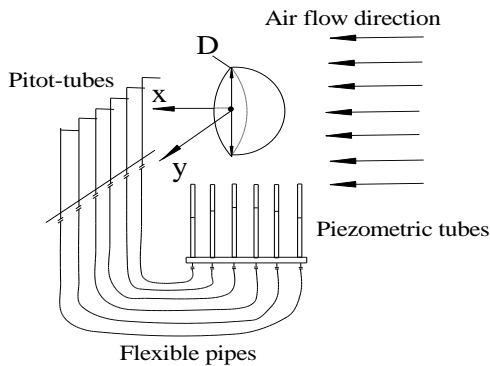


Fig. 1. Schematic representation of the wake pressure measurement apparatus.

For the air flow mean velocity of 17.25 m/s, the pressure reduction in dimensionless form as the pressure coefficient, is indicated in Fig. 2.

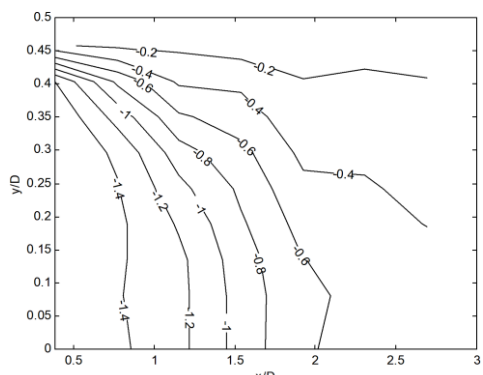


Fig. 2. Pressure coefficient distribution at the leeward of a semi-spherical surface.

It is seen from this figure that an adequate pressure reduction is formed at the leeward of the surface especially at short distances.

Having confidence from the pressure reduction within the wake, a large-scale experimental set up was established. A variable speed axial fan having 60 cm diameter was installed inside an opening located at the lower part of a side wall of a cubical enclosure. Another opening, $0.65 \times 0.45 \text{ m}^2$, was created at the upper part of the same side wall. One smooth pipe having 10 cm diameter and 60 cm length was fixed vertically on a support in front of the upper opening. The top end of the pipe was adjusted to be at 30 cm distance from the centre point of the opening. A support was fixed at the top end of the pipe by which a solid surface could be kept at an arbitrary position between the opening and the pipe. A number of circular plates and semi-spherical surfaces having different diameters ranging from 15 to 30 cm were made from plastic sheet with about 2 mm thickness. Each of the solid surfaces could be mounted on the support in turn in the experiments. A bell-shaped connector was also attached to the bottom end of the pipe to direct air flow from the surroundings into the pipe. One small opening was also formed on the pipe, through which, the air velocity could be measured at different points within the pipe and close to the bottom end using a probe anemometer (Testo, 0-20 m/s, $\pm 0.03 \text{ m/s}$). A schematic illustration from the

test rig is seen in Fig. 3.

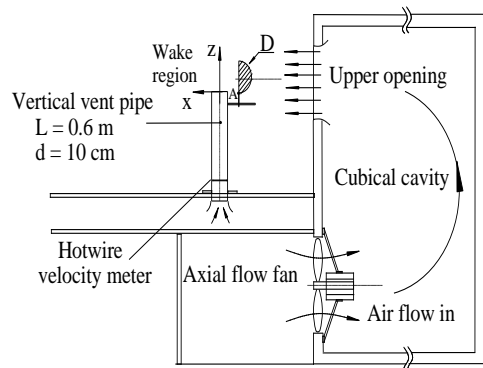


Fig. 3. Schematic representation of the test rig.

When the fan was turned on at a predetermined rotational speed, an air flow was directed into the surroundings through a short duct connected to the upper opening. In order to examine the air flow specifications, normal velocity component was measured on the vertical symmetry line located at different distances from the opening using a mini CTA hotwire probe. A representative velocity distribution is shown in Fig. 4 in which the mean flow velocity is about 2.25 m/s.

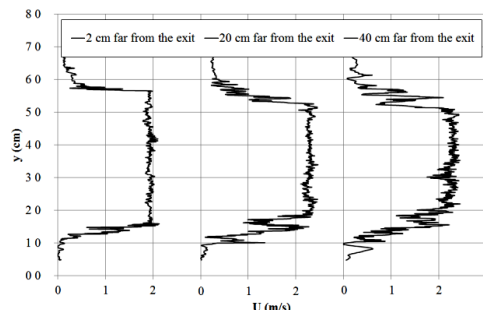


Fig. 4. Air flow velocity distribution at different distances from the exit of the duct.

It is seen from Fig. 4 that the main flow is almost uniform at short distances from the exit of the opening and a thin shear layer exists at the sides of the flow. The shear layer develops gradually at the sides as the flow is getting far from the opening, but the uniform flow persists at the core region for the examined distances from the opening. It is worth nothing that the mean flow velocity at the core region increases slightly as the flow is developed. This trend is quite similar to the flow discharging from an orifice in which a contracted area occurs at a short distance from the exit where the maximum flow velocity is measured. A similar velocity distribution was also obtained for the horizontal symmetry line. Having determined the air velocity distribution, the solid surface on the support was so adjusted to be within the main flow in all the experiments.

Each of the solid surfaces, disk or semi-sphere, was fixed on the support of the vent pipe in turn and it was positioned at a prescribed location to produce a wake where the top end of the pipe was within this region. The bottom end of the vent pipe was always within the stagnant surroundings. Due to the

pressure difference across the pipe an induced air flow was established within the pipe. The velocity of the air flow entering the pipe, which was a nearly uniform flow, was measured at several points based on which the air flow rate was determined for different configurations examined in the experiments.

3. RESULTS

The experiments were conducted using semispherical surfaces and also simple circular plates. The results of the experiments as the rate of air through the vent pipe are presented in the following subsections.

3.1 Using Semi-Spherical Surfaces

At the first stage of the experiments, semi-spherical surfaces having different diameters ranging from 15 cm to 30 cm was mounted in turn on the support. According to the coordinates defined in Fig. 3, various geometrical configuration was specified using x and z Cartesian coordinates. These two axes were fixed at the top centre point of the vent pipe and the coordinates of the top of the support denoted by 'A' were used to specify the geometrical configuration. For the case of $x = -d/2$ and $z = -0.05$ m, Fig.5 presents the ventilation rate through the vertical pipe measured at different airflow velocities.

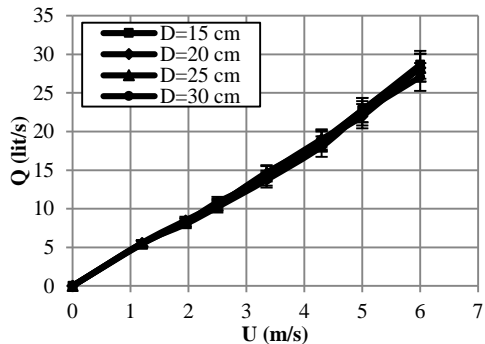


Fig. 5. Ventilation rate resulted for semi-spherical surfaces ($x = -d/2$, $z = -0.05$ m).

It is seen that the ventilation rate steps up linearly as the flow velocity is increased, where the size of the semi-spherical surface has a very negligible effect on this parameter. Fig. 6 shows a typical of the examined configurations in which $x = -d/2 - 0.10$ m, $z = -0.10$ m. It is observed that the ventilation rate is considerably lower compared to the previous case and the effect of the size of the semi-spherical surfaces is quite evident for this geometrical configuration. It could be concluded that to achieve effective ventilation rate, the top end of the vertical pipe should be well placed within the wake produced by the semi-spherical surfaces.

Uncertainty analysis has also been performed and error bars have been plotted on the graphs. It is seen that the uncertainty in the ventilation rate is increased for the larger amounts of the air flow velocities for which the flow fluctuations are

increased.

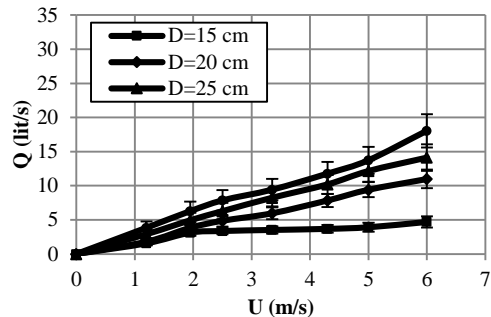


Fig. 6. Ventilation rate resulted for semi-spherical surfaces ($x = -d/2 - 0.10$ m, $z = -0.10$ m).

3.2 When Using Circular Plates

At the second stage of the experiment, semi-spherical surfaces were replaced by circular plates having the same diameters and the experiments were repeated. Fig. 7 shows the ventilation rate obtained at different wind velocities and for the geometrical configuration of ($x = -d/2$ and $z = -0.05$ m). It could be seen that similar to the result of the last geometry, ventilation rate increases linearly with the wind velocity and almost independent of the size of the circular plates. However, the ventilation rate is slightly greater than that of the previous geometry for the same wind velocity and the same diameter of the surfaces. Also, it could be observed that the induced flow within the vertical pipe is somewhat stable for the case of the semi-spherical surfaces. Fig. 8 presents the ventilation rate obtained for the circular plates employed at geometrical configuration of ($x = -d/2 - 0.10$ m, $z = -0.10$ m).

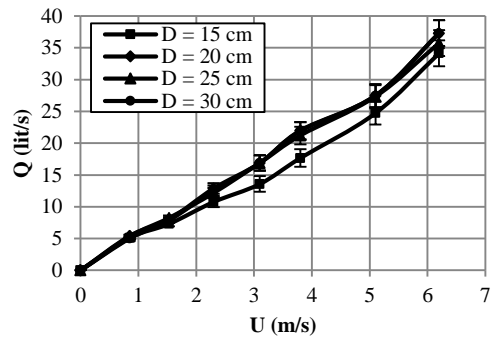


Fig. 7. Ventilation rate resulted for circular plates ($x = -d/2$, $z = -0.05$ m).

Unlike to the previous geometry, it is seen that except for the smallest plate, the ventilation rate has a very small decrease at this geometrical configuration. This trend indicates that the wake region produced by a circular plate has more extension and strength compared to that of a semi-spherical surface having the same diameter. It is worth nothing that the error bars are also slightly greater than those of the semi-spherical cases presenting larger flow disturbances at these cases.

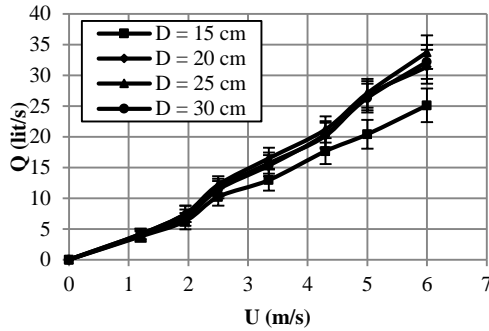


Fig. 8. Ventilation rate resulted for circular plates ($x = -d/2-0.10$ m, $z = -0.10$ m).

4. DISCUSSION

Ventilation rate caused by a semi-spherical surface and a circular plate both having 20 cm diameter and for the geometrical configuration of $x = -d/2$ and $z = -0.05$ m is shown in Fig. 9. Ventilation rate produced by the vertical pipe itself with no additional surface attached on the support is also seen in this figure. The figure presents that the ventilation rate produced by a vertical pipe itself could be at least doubled by using a simple geometrical surface as outlined in the previous section.

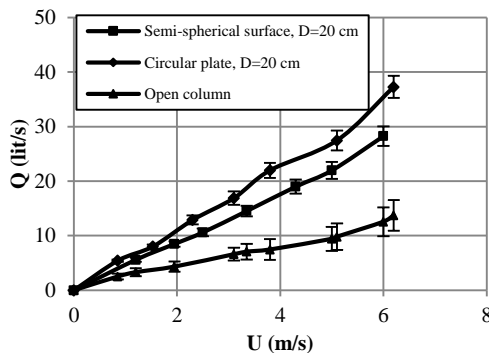


Fig. 9. Comparison of the ventilation rates of different geometries ($x = -d/2 - 0.10$ m, $z = -0.10$ m).

In order to indicate the significance of this conclusion, ventilation rate reported by Khan *et al* (2008) has been reproduced in Fig. 10. In this figure ventilation rate through a 250 mm open column has been compared with those of two different vent hats and a turbine ventilator attached on the top of the open column at different wind speeds. It can be seen from this figure that the ventilation rate achieved by a turbine ventilator is quite comparable with that of an open column. Whereas, two other geometries i.e. plane baffle and Chinaman's hat both have lower ventilation rates than the turbine ventilator. Although the open column itself may not be a practical means of ventilation due to the lack of weather tightness, but it could be used as a reference to make a comparison between the results. In addition, it could be worth nothing that while the ventilation rate achieved by a turbine ventilator is quite comparable with that of an open column, it could be nearly doubled by using the wake region

produced by a simple solid surface.

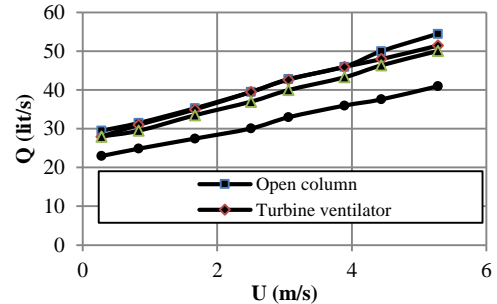


Fig. 10. Comparison of 250 mm turbine ventilator to an open column and two vent hats (Khan *et al.* 2008).

Ventilation rate achieved by the method described at the present study might seem not to be intensive enough to be applied in the ventilation of buildings. However, based on a similarity analysis it could be shown that the ventilation rate could be increased linearly by enlarging the size of the vent pipe. Two dimensionless parameters such as:

$$\begin{aligned} \Pi_1 &= UD/\nu \\ \Pi_2 &= U/V \end{aligned} \quad (1)$$

should be taken into account for the flow field to be similar in geometrically similar configurations. Ventilation rate achieved by any arbitrary size of the vent pipe, Q , could be expressed as:

$$Q = Q_0(D/D_0)^2(V/V_0) \quad (2)$$

in which, the reference parameters have been denoted by subscript '0'. Assuming constant physical properties for air and substituting similarity dimensionless parameters defined in Eqs. (1) into Eq. (2) then gives:

$$Q = Q_0(D/D_0) \quad (3)$$

This equation suggests that for any prescribed wind velocity, the ventilation rate achieved by a vent pipe is proportional to the size of the pipe under geometrically similar configurations.

Based on the results of the present study, it was also cleared out that more stable flow could be achieved when using semi-spherical surfaces. In order to compensate for the wind direction, the semi-spherical surface along with one small vertical wing could be mounted on a bearing attached to the top end of the vertical pipe. The wing, being at the opposite side of the semi-spherical surface, would be always at the downwind direction positioning the surface in front of the wind. Therefore, the top end of the vertical vent pipe would be within the wake region generated by the semi-spherical surface.

5. CONCLUSION

It is concluded that the separated flow and the wake regions occurring at the leeward side of a solid surface, such as a semi-spherical surface or a circular plate, have the potential use in wind-induced ventilation. Ventilation rate achieved by an open column could at least be doubled positioning the top end of the vertical pipe or channel within the

wake region. More stable ventilation flow would be established using a semi-spherical surface to a circular plate. Utilizing one small vertical plate as a wing at the opposite side of the surface, both mounted on a bearing and attached to the top end of the vent pipe, could relatively compensate for the wind direction.

REFERENCES

- Adekoya, L. O. (1992). Wind energy end-use: The performance characteristics of a rotating suction cowl. *Renewable Energy* 2(4-5), 385-389.
- Aldawoud, A. and R. Clark (2008). Comparative analysis of energy performance between courtyard and atrium in buildings. *Energy and Buildings* 40(3), 209-214.
- Chiu, Y. H. and D. W. Etheridge (2007). External flow effects on the discharge coefficients of two types of ventilation opening. *Journal of Wind Engineering and Industrial Aerodynamics* 95(4), 225-252.
- Chu, C. R., Y. H. Chiu and Y. W. Wang (2010). An experimental study of wind-driven cross ventilation in partitioned buildings. *Energy and Buildings* 42, 667-673.
- Haw, L. C., O. Saadatian, M. Y. Sulaiman, S. Mat and K. Sopian (2012). Empirical study of a wind-induced natural ventilation tower under hot and humid climatic conditions. *Energy and Buildings* 52, 28-38.
- Hughes, B. R. and M. Cheuk-Ming (2011). A study of wind and buoyancy driven flows through commercial wind towers. *Energy and Buildings* 43, 1784-1791.
- Karava, P., T. Stathopoulos and A. K. Athienitis (2007). Wind-induced natural ventilation analysis. *Solar Energy* 81(1), 20-30.
- Khan, N., Y. Su and S. B. Riffat (2008). A review on wind driven ventilation techniques. *Energy and Buildings* 40, 1586-1604.
- Khan, N., Y. Su, S. B. Riffat and C. Biggs (2008). Performance testing and comparison of turbine ventilators. *Renewable Energy* 33, 2441-2447.
- Lai, C. M. (2006). Prototype development of the rooftop turbine ventilator powered by hybrid wind and photovoltaic energy. *Energy and Buildings* 38, 174-180.
- Li, L. and C. M. Mak (2005). The assesment of the performance of a wind catcher system using computational fluid dynamics. *Building and Environment* 42, 1135-1141.
- Mak, C. M., J. L. Niu, C. T. Lee and K. F. Chan (2007). A numerical simulation of wing walls using computational fluid dynamics. *Energy and Buildings* 39, 995-1002.
- Mochida, A., H. Yoshino, H. Takeda, T. Kakegawa and S. Miyauchi (2005). Methods for controlling airflow in and around a building under cross-ventilation to improve indoor thermal comfort. *Journal of Wind Engineering and Industrial Aerodynamics* 93(6), 437-449.